DNA Condensation with Two-Sided Bridging Proteins

Jason Klebes

December 4, 2015

0.1 Abstract

The condensation of DNA and chromatin into organized compacted states follows through a variety of binding proteins of various sizes and geometries. A model polymer and an environment of dimer binding proteins, represented by a body with two attractive atoms around a central atoms, were simulated to examine the effects of this shape of protein body on polymer condensation at various concentrations. As expected, polymers with characteristics of DNA or chromatin are compacted at sufficient concentrations and potential strength of the proteins, with chromatin forming a dense globule and DNA forming various formations of parallel strands. In experimental and theoretical models with ionic ligands, a compacted state at moderate concentration and a return to the uncompacted state at high concentrations has been observed. However, the predicted second stable state was not observed in the simulation, indicating that it is not caused solely by occupation of binding sites.

0.2 Introduction

In eukaryotes as well as prokaryotes, DNA is stored in a highly compacted form, condensed both at DNA levels into a chromatin fiber and packed into the small nuclear space at the chromatin level. Because unfolding and refolding both during cell division and for transcription takes place within small timescales, a highly dynamic and ordered mechanism is needed [1]. The structuring and compaction as well as the resulting regulation of gene expression is mediated by a variety of proteins such as histones in eukaryotes or IHF, FIS, and H-NS in bacteria [2]. A variety of sizes and geometries of DNA structuring proteins exist. In this project a structure similar to H-NS, which is known to form dimers with two binding regions and a flexible middle region [1], is considered.

H-NS has been shown to form clusters of bridging connections between two isolated strands of DNA *in vitro* [3], although the effect on a free polymer in solution as well as interacting with other proteins may differ. Because *in vivo* observations of the proteins' interaction at a molecular level are not readily attainable, simulation of a model polymer can be used to predict effects in a more realistic and dynamic environment.

We simulate the interactions between a polymer representing DNA or Chromatin polymer and number of bridging protein molecules, represented as double-sided rigid bodies. Questions to explore are the effect of different concentrations of these proteins on the size and structure of the compacted DNA polymer, and explaining the effects in view of binding behavior of the double-sided proteins. In particular, the protein was expected to cause condensation at moderate concentration but a return to unfolded states at sufficiently high concentrations.

0.2.1 Concepts

Both DNA and chromatin fiber are polymers, the dynamics and characteristics of which may be described in terms of length, diameter, bending rigidity, and persistence length. A polymer may be modeled as a chain of N rigid segments of length l. In the simplest model, the angle between two segments is completely flexible and completely random and the polymer does not interact with itself. To model a somewhat stiff chain, the angle between two segments is correlated with the angle of adjacent segments. [4] This

corresponds to a chain of randomly oriented segments of the Kuhn length l_k, the length at which the correlation with the angle is lost. Taking the limit of the Kuhn chain of length L with infinitely many small segments we get the continuous worm-like chain model. The persistence length L_p, at which the orientation is uncorrelated, depends on the bending rigidity constant κ_b as well as the energy supplied by the thermal environment as

$$L_p = \frac{\kappa_b}{kT}$$

[4] . For DNA, the persistence length is about 50 nm (or 20 in units of $\frac{\sigma_{DNA}}{kT}$), for chromatin it is about 90nm (3 in units of $\frac{\sigma_{chromatin}}{kT}$). While the absolute persistence length of chromatin is greater, it is more flexible in relation to the polymers' respective diameters σ of 2.5nm and 30nm.

In this simulation, the positions of chain and protein bodies must be evolved according to particle interactions as well as stochastic environmental effects. The dynamics of a system of particles in an environment of potentials exerted by other atoms and an implicit solvent are described by the Langevin Equation

$$M\ddot{X}(t) = -\nabla E(X(t)) - \gamma M\dot{X}(t) + R(t)$$

. The first contribution is the sum of potentials of other bodies, the second term is a inertial effect of the solvent according to Stokes' law $\gamma = 6\pi\nu a/m$, and $R(t)$ represents random impulses from solvent molecules [5, p. 480].
Numerically solving a system of second-order differential equations - as is needed to relate forces to position - is done by Verlet integration, a simple and stable numerical method. For example, in the position Verlet variant, each new position is derived from previous positions X_n, X_{n-1} and an estimate of forces resulting from previous positions $\tilde{F_n} = \tilde{F}(X_n)$ as

$$X_{n+1} = 2X_n - X_{n-1} + \Delta t^2 \tilde{F}_n$$

[5, p. 449-455] To efficiently simulate a large system of particles, this can be modified in various ways, such as treating more slowly changing long-range forces in less detail than short-range interactions. Different Verlet methods (their suitability depending on parameters such a γ) can then be applied to the discretized Langevin equation. [5, p. 472-484]
In this project, the simulation was run with LAMMPS, a molecular modeling software by Sandia National Laboratories [6]. It solves the above dynamics with the velocity Verlet variant through serial or parallel processing of small regions of atoms.

0.3 Model

In this model, the DNA polymer is represented as a string of discrete "beads" connected by finite extensible nonlinear elastic (FENE) bonds. These resist both length and angular deformation with a given force. In the radial direction, the potential consists of an attractive term and the repulsive part of a Lennard-Jones potential.

$$E = -.5KR_0^2 ln(1 - (\frac{r}{R_0})^2) + 4\epsilon((\frac{\sigma}{r})^6 - (\frac{\sigma}{r})^{12}) + \epsilon$$

The potential between non-adjacent polymer particles is another Lennard-Jones potential cut off at its minimum ($r = 1.22\sigma$) so that solely the repulsive part remains. This represent the spatial extent of the particles; they behave as spheres which cannot overlap rather than as point particles .

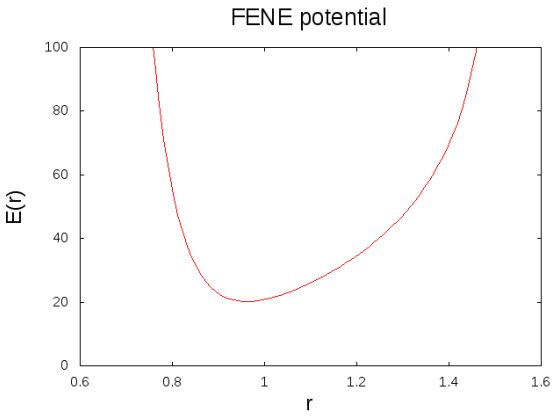

Figure 1: Shape of FENE potential

In contrast to previous approaches, the protein is modeled as a rigid body comprised of three "atoms". The two outside beads interact with DNA beads attractively via a Morse potential, while the middle body repulses DNA beads, ensuring the molecule will not connect in parallel to the same polymer strand but stand off it, leaving the other attractive end free to connect with another section of the polymer. In addition to the number of proteins, the strength and shape of the attractive potential can be varied.

Figure 2: Representation of polymer and protein bodies in initial state

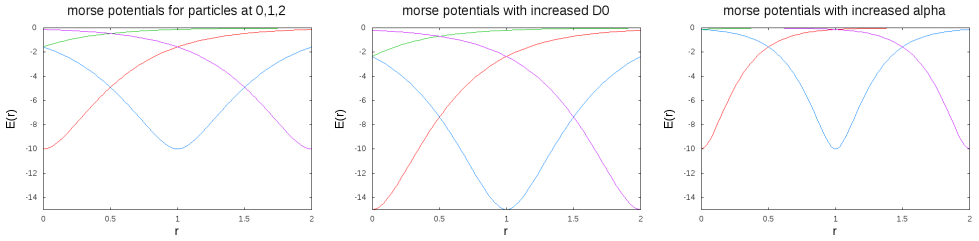

A greater potential depth leads to stronger and longer-lasting interactions, while a shallower shape enables proteins to move from one polymer bead to the next.
The attractive force is short ranged; protein bodies must pass closely by the polymer in their random paths through the solvent to become bound. When bound to the polymer, solvent forces act on the proteins and may cause them to become detached from the polymer. Depending on the strength of the binding potential, an equilibrium number of proteins attached will result.
It is predicted that few attached proteins result in some bridges between sections of the polymer, forming loops, while more will condense into a compacted shape, and an over-abundance of proteins will possibly render it unable to connect again as all sections of the polymer are already occupied.

LAMMPS is set to evolve the model using Langevin dynamics, which includes a forces representing solvent effects. The Brownian motion is assumed to be completely random; hydrodynamic effects are neglected. The drag coefficient γ as well as the solvent temperature are specified in the script.

The relevant time scales of the simulation follow from these properties of the environment: units are given in the Lennard-Jones time, while dynamics should be considered relative to the Brownian time, the average time in which a particle moves by its own length, given by

$$\tau_B = \frac{\sigma^2}{D}$$

with diffusion coefficient

$$D = \frac{k_B T}{\gamma}$$

Here, this is set via diameter $\sigma = 1$ and drag coefficient $\gamma = 2$ to be $\tau_B = 2$ (in LJ units). This does not correspond to a realistic relationship between these values, but the fundamental dynamics of the system are conserved when scales are adjusted to yield observable results within the simulated timespan.

The simulation is confined to a box with periodic boundary conditions. Particles crossing the box boundary return to the box on the other side, conserving the number of atoms in the simulation and confining them to the space of interest.

0.4 Methods

Computer simulation and data analysis with various software and programs was used to explore the effects of introducing this model of proteins on the DNA polymer. The evolution of a DNA polymer with proteins in a solution was run using LAMMPS. An initial configuration of randomly generated particle positions is generated with a C++

program. A script of "soft" potentials is first applied to separate overlapping atoms before runing the main simulation. After running the LAMMPS simulation, a Java program reads and analyzes the resulting output files. VMD was used to visualize snapshots of the molecules' configuration over time.

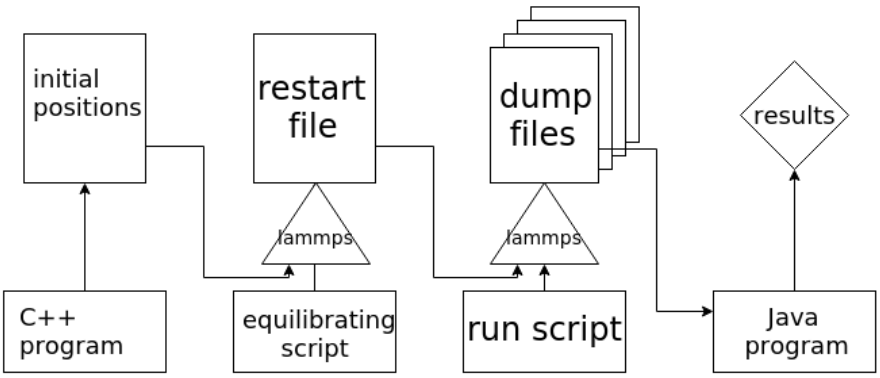

Figure 3: procedure

0.4.1 Simulation

The provided C++ program "generate_DNA_proteins.cc" randomly generates particle position for polymer length, protein number, box size, and protein type (0, 1 or 2 attractive atoms attached to the central atom) specified by user input. Particles are generated in their respective chain or bodies but not checked for overlap.
This is corrected for by running the equilibrating LAMMPS script on the initial conformation. Here, the particles are pushed apart by a series of increasingly strong interaction types. If overlapping particles were immediately subjected to FENE potentials, the strong repulsive force at the short distance would break the bond.
The output of the equilibration process consists of a single restart file, from which the 'run' LAMMPS script is started.

The core LAMMPS script to evolve the model over time consists of reading initial positions from restart file; grouping atoms into types; setting bond types and parameters between groups; specifying the time interval of writing to dump file and thermo files; and the command to run the model a given number of steps.

Several choices of parameters must be made in the script. These were refined over several attempts at running the simulation to compromise between realism and functional results.
The polymer representing DNA or chromatin must be long enough so that it can interact with itself, condense, and form loops for a given flexibility, while being small enough to compute and small relative to the box to not interact with itself over the periodic boundary.

Chromatin and DNA polymers differ in the bending rigidity parameter, set as 20 and 3 $\frac{\sigma}{kT}$ respectively.
The box must be small so that proteins are dense and have a high chance of interacting with the polymer, but not so small that the polymer interacts with itself across the box boundary. A polymer size of 300 beads and a box size of 100 x 100 x 100 were chosen.
For all simulations, a polymer chain consisting of 300 beads is used.
The protein-polymer Morse potential is initially chosen to be highly attractive with potential depth $D_0 = 18$. An equilibrium state between proteins attaching and detaching due to solvent interaction can thus be reached within the simulated timeframe and the effects of most available proteins attaching to the DNA can be seen. α is initially chosen as 3.25, making it unlikely a protein will slide to the next polymer particle.
The timestep is chosen to be .005 (in Lennard-Jones units/timescale). With the initial estimate of .01, polymer particles near an attractive protein molecule were moved too close together during one timestep, causing strong repulsive forces from the FENE bonds to break the polymer chain. The choice of timestep must compromise between simulating a long enough length of time to observe particle movement and effects and stability on each successive step of numerical integration.

Inserting a loop around the LAMMPS script, with the variable of interest calculated from loop number, generates a set of dump files for runs with these different conditions. The quantity varied may be attractive forces between polymer, depth D_0 or sharpness α of attractive potential between proteins and polymer, or number of proteins n_p. To avoid generated and equilibrating a new restart file for each different number of proteins in the latter case, these are varied by deleting varying numbers of protein bodies from the initial number.

Coordinates of polymer and protein bodies as well as thermodynamic variables are written to files at regular intervals.

VMD (Visual Molecular Dynamics) is a software which displays a 3D image of the particles in space from the file of positions [7]. It was used to confirm the intended behavior of the polymer and proteins in the simulation and gain insight into results. For example, it can show the scale of the movement of particles between one output and the next, whether proteins are binding to the polymer, and conformations of the bound polymer.

0.4.2 Analysis

The radius of gyration quantifies the spatial extent or compactness of a molecule: it gives the root mean square distance between each point and the molecule's center of mass.

$$R_{gyr}^2 = \frac{1}{N}\sum_{i}^{N}(r_i - \bar{r})^2$$

A Java program was written to analyze the position and thermal dump files for the values of various variables, such as R_{gyr}, e_{pair}, $n_{attached}$. The program consists of "Coordinate", "Frame", "Polymer", "Correlation", and "RunCorrelation" classes.
The Frame class contains methods to read in all lines in a given dump file and store them

in an array; read in the number of atoms and therefore size of a frame from the dump file; read coordinates comprising the next timestep/frame from the array of lines and analyse this before reading and processing the next frame. The methods work on a sequential basis: nextFrame() copies the first set of coordinates from the list of lines to the arrays of location values (overwriting the last set) and deletes it from the beginning of the list of lines. The alternative approach of obtaining any specified frame from the middle of the dump file text by trimming beginning lines was far more time consuming. Positions within the box and the number of times a particle has crossed the periodic boundary are read in, arrays of both "raw points" (coordinates within the box) and "image points" (in the unwrapped space) are stored. The former are used to analyse protein interactions with the polymer, the latter for the extent of the polymer in space, which may cross the box boundary. While coordinates are given in the dump files in units such that the size of the box =1, they are converted back to LJ units where the diameter of a particle =1. The class contains methods which calculate variables such as mean polymer position, radius of gyration, or number of proteins attached for the single frame from the list of coordinates.
The class Polymer represents a single polymer with proteins over time, i.e. the set of Frame objects read from a single dump file. It contains methods which loop over Frame, reading in each next section of the dump file, initiating its arrays, and analyzing for the variable of interest and storing it as an array of values over time. It can then calculate an average over time of the variable in a given time range.
The class Correlation contains various methods which call the appropriate methods in Polymer on a set of dump files and generate two columns of the chosen variables in each dump file.
Analysis retains the Lennard-Jones units of the simulation.

0.5 Results

Areas explored were the formation of a polymer under varying number of protein molecules, the limit of oversaturating the polymer, and varying the attractive potential.

0.5.1 Compaction at varying concentrations

After running the simulation for some time, an equilibrium number of proteins attached will form depending on the balance between the attractive force between proteins and the polymer and impulses from the solvent which can detach a protein. The depends on the number of proteins available and the depth of the potential D_0. The polymer's radius of gyration, as well the number of proteins attached were calculated for sets of simulations with varying numbers of proteins. The thermodynamic variable pair energy directly corresponds to the number of protein-polymer bonds formed.
The first attempt (with box size 500 x 500 x 500) showed little interaction between proteins and DNA because the box size chosen was too large. The proteins were distributed throughout the box with low density, making it unlikely that they would pass close by a DNA bead and interact with it. However, with a higher density in a box size 100 x 100 x 100, the gyrational radius of the polymer clearly decreases from the initial number to fluctuating about a lower value.
To determine when an equilibrium configuration is reached, the gyrational radius of a

single run with a set number of proteins is first tracked.

From this data (Figure 4), the time span 500 to 1200 frames is chosen to evaluate the average value over time $< R_{gyr}(t) >$ of the final radius.
The simulation was then run multiple times for different numbers of protein bodies from 0 to 200. High concentrations up to $n_p = 200$ were included as resolubilization behavior was expected at this limit. A high attractive force $D_0 = 18k_BT$ was initially chosen to reach the stable final state within the simulation time. The following relationships $< R_{gyr} > (n_p)$ were obtained (Figure 5, Figure 6), where radius of gyration is plotted both against the total number of protein bodies in the simulation and against the number of times an outer protein atom was found to lie near a polymer atom - twice the number of bridges formed if all proteins are attached on both sides. Also plotted (Figure 7) are number of connections and e_{pair} - total potential energy of the system - number of proteins available, shown here for chromatin.

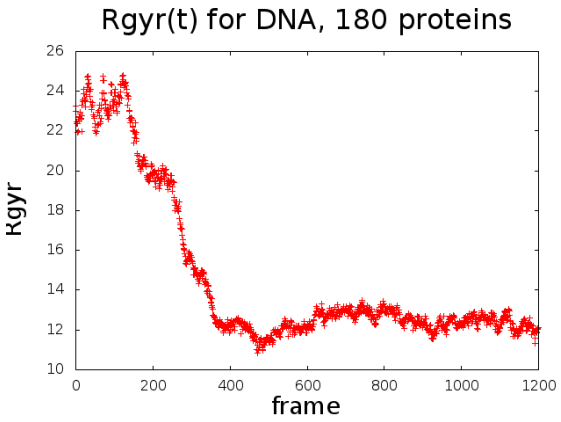

Figure 4: Radius of gyration of a compacting DNA polymer over time

In both cases it is clear that at a low threshold concentration of proteins the polymer

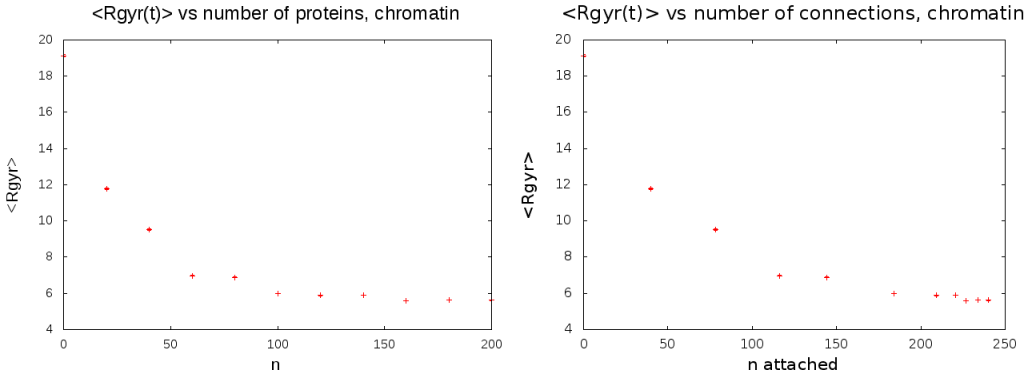

(a) (b)

Figure 5: Radius of gyration of chromatin by number of available bridging proteins and by number of attached bodies

transitions to the condensed state, and remains in this state for all higher concentrations. A qualitative and quantitative difference between chromatin and DNA is apparent from the data: the more flexible chromatin polymer transitions more gradually through partially compacted states and attains a lower final radius of gyration, while the DNA

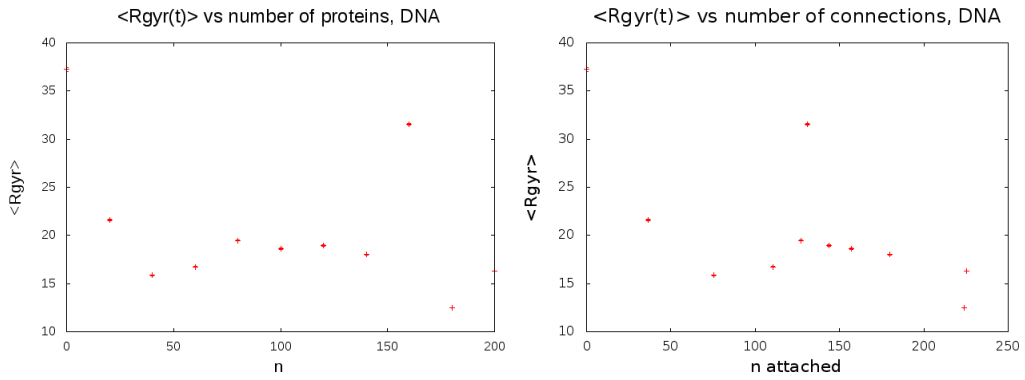

Figure 6: Radius of gyration of DNA polymer by number of available bridging proteins and by number of connections

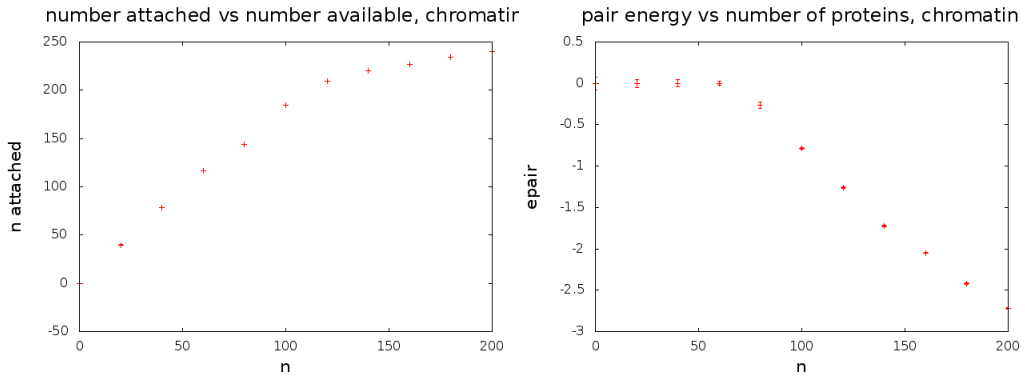

Figure 7: Number of connections and total energy of connections by number of protein bodies available

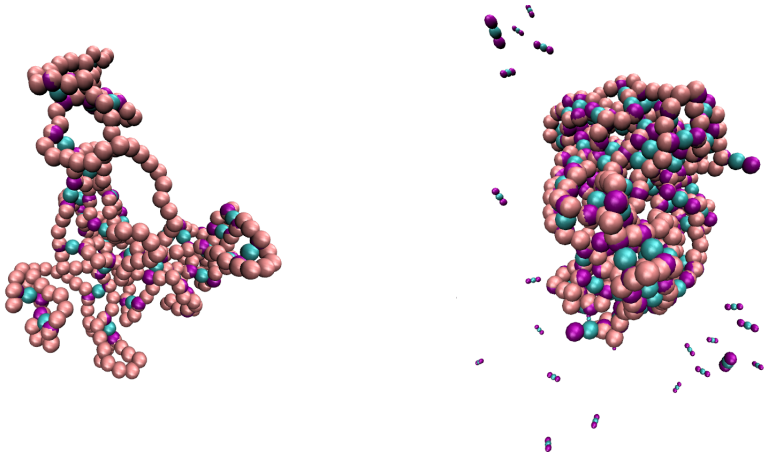

(a) Chromatin with 20 proteins (b) Chromatin with 160 proteins

Figure 8: Partially compacted and maximally compacted chromatin polymer

polymer has a less compacted and more variable final radius of gyration but assumes this formation even with few bridges. Further details of their different folding behaviors can be seen when visualizing the molecule.
As observed in similar simulations with single-bodied proteins [8], the chromatin first forms several loops, then condenses into a highly compacted and uniform final state (Figure 8) for increasing protein concentrations.
For DNA, proteins connect polymer strands in a ladder-like fashion, forming circular or linear configurations (Figure 9). Past a threshold around 40 proteins, the structure is not altered by the availability of more proteins to form denser rows of parallel bridges. However, the polymer randomly falls into more of less distributed shapes. The possibility of compacting into either circular or rod-like structures is known from experiments, where observed type of structure has been found to be modulated by ions and other molecules in the solvent [9]. In this simulation the polymer remains in a single configuration once folded, leading to a value of $< R_{gyr} >$ with little deviation over time that does not accurately correspond to the possible deviation in compactness for this number of proteins. For more accurate data, an average over $< R_{gyr} >$ from multiple runs should be averaged.
The outlier represents a case where a large straight segment of the DNA polymer accumulated protein bodies but did not pass close to another free strand and connect during the simulated time. The simulated polymer is short in comparison to the persistence length of the stiffer DNA, it is expected to be more likely to connect of a longer DNA body were available.
The more flexible chromatin does not form the structures like DNA because it starts folding at multiple points, leading to small structures instead of the possibility of a global linear or circular pattern.

0.5.2 Dependence on attractive potential

To further explore the stability of the equilibrium configuration, the average time a single protein is attached was probed by tracking 10 single-sided proteins interacting with the

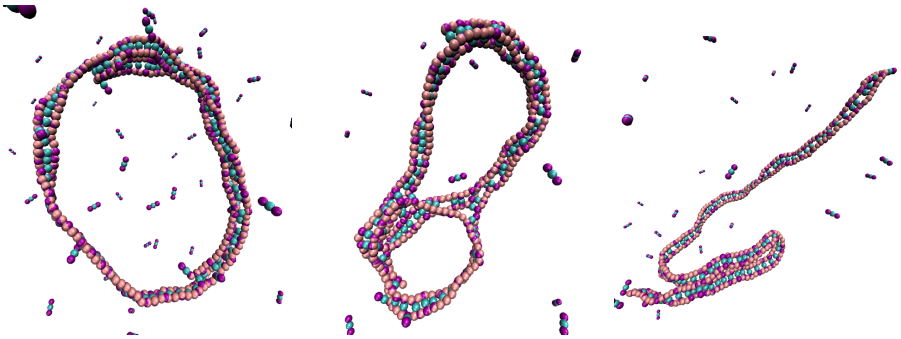

(a) (b) (c)

Figure 9: Variation in maximally bridged DNA polymer structure

polymer. The result is an exponential relationship between duration of a single attachment and attractive force D_0 (error bars are larger as longer attachment times lead to fewer attachments during the simulated time period).

This run, using almost isolated single-sided protein molecules, does not entirely reflect the time a double-sided protein held in a ladder-like configuration between two strands of polymer by other proteins stays attached.

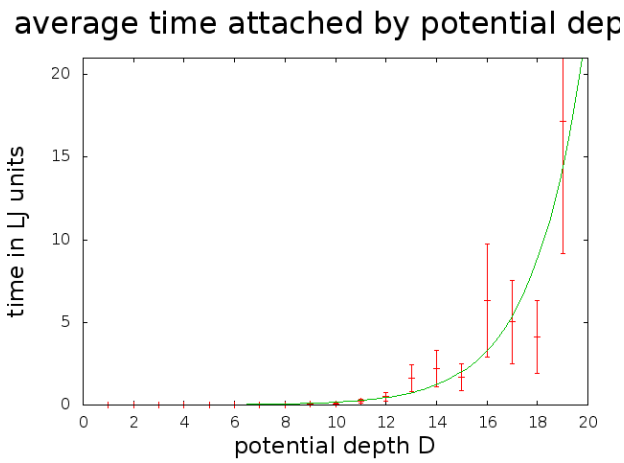

Figure 10: Exponentially longer average attachment times for isolated single-sided proteins

From established models, varying D_0 is expected to result in similar behavior as varying n_p: the polymer sharply transitions between an open phase and a compacted phase at a threshold value of both number of proteins and strength of binding [9]. This agrees well with the observed characteristic of the simulation that the desired $R_{gyr}(n_p)$ relationship cannot be observed at lower values such as $D_0 = 10k_BT$ or $D_0 = 12k_BT$, while these results are similar for values such as $D_0 = 15k_BT$ and higher.

The relationship $< R_{gyr} > (n_p)$ was again explored at $D_0 = 15k_BT$ - the number was chosen because a small decrease from $D_0 = 18k_BT$ leads to a sufficiently large decrease in average time attached of isolated proteins. However, as predicted from two-state models, the resulting condensation behavior with varying number of proteins is nearly identical.

0.5.3 Resolubilization

Based on experimental results [10], a second stable equilibrium state was expected to emerge at high concentrations of bridging proteins.
The expected phenomenon - that above a certain high number of proteins the polymer would become saturated and unable to form connections, leading to a return to higher R_{gyr} - was not observed for protein numbers up to 200. Visualising the compaction process in VMD, it can be seen that a protein will form an initial bridging connection around which subsequent proteins will preferably connect, forming a growing area of stable bridges and "zipping up" the polymer.

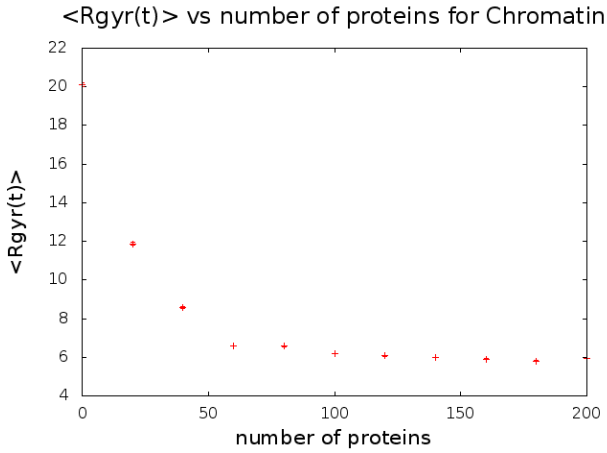

Figure 11: Similar compaction behavior with attractive potential reduced to $D_0 = 15k_BT$

To observe the predicted second uncompacted stable state at high protein concentration, a simulation was run in two parts. First, solvent interactions moving the polymer were disabled while a large number of proteins ($n_p = 400$, with box size decreased to 50 x 50 x 50) with strong attractive force ($D_0 = 50k_BT$) are allowed to connect to the polymer. Once the polymer is fully occupied with singly-connected proteins, it is run under normal conditions ($D_0 = 18k_BT$ and allowed to move). This alternative initial state was predicted to correspond to a second stable equilibrium minimizing energy; the polymer is therefore expected to remain in this state. However, stability of the coated, non-globular state was not observed: proteins quickly detach, and reattach as the usual bridging connections (Figure 12).

The effect was similarly not observed in an even more extremely oversaturating environments of 600 proteins (in 50 x 50 x 50 length units); with more than 700 proteins the concentration and forces become too large to track particles. When continuing with an extremely strong attractive force ($D_0 = 50$), along with the large number of proteins (400) and initial coating, connections form only in few places. The situation - where solvent impulses were rendered negligibly small compared to other intermolecular forces- is not a realistic model and even in this case an equilibrium compacted state would eventually result. No evidence for a coated, unconnecting equilibrium state was found even under extreme conditions.

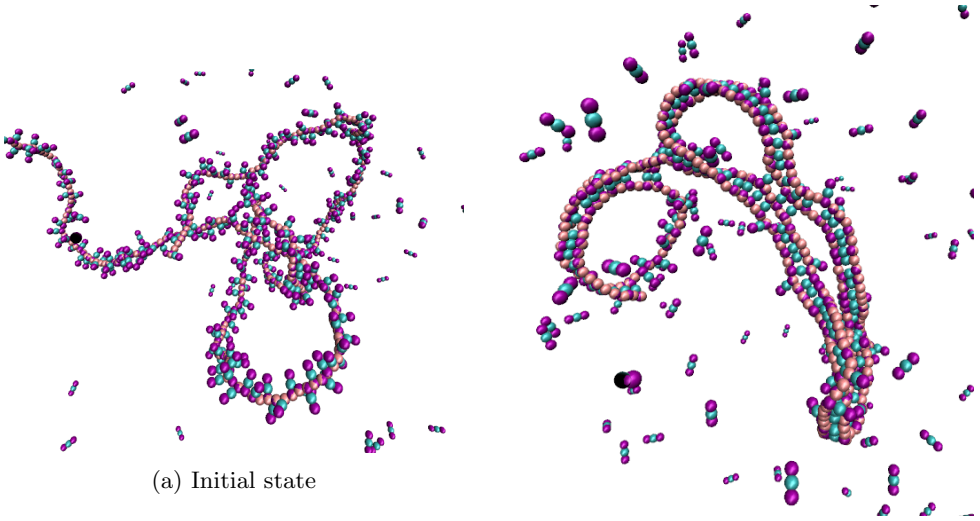

(a) Initial state

(b) After 100 frames

Figure 12: Evolution of DNA polymer from coated state

0.6 Discussion

Results obtained show globular compaction of chromatin and circular or rod-like compaction of DNA polymers. Qualitatively these correspond well to expected effects at moderate protein concentrations despite the simplified model.
The results could be refined by simulating a large number of runs. In this project, the average gyrational radius of a few single runs, in which the polymer compacted into one stable formation, was examined. To obtain a more accurate quantification of average size of the molecule, averaging over the many possible conformations would be needed.
In addition, the different structures (double strands, circles, three-strand connections...) the DNA or chromatin fiber forms are itself an important area of further study. The varieties and frequencies of different conformations as a consequence of few or many bridging proteins, as well as their stability and evolution, are highly relevant to DNA superstructure.
While no direct protein-protein forces were included, cooperative effects of adjacent bridge formation and greatly stabilized binding emerged.

The lack of the expected resolubilization and second stable equilibrium indicates that other factors, rather than solely of all binding sites by proteins, are responsible for this effect in experiments. Several factors not included in this simulation are hypothesized to contribute, such as electrostatic effects between coated polymer strands or osmotic pressure of explicit solvent molecules [9]. Another difference to experiments is that these were carried out with small, ionic ligands. Electrostatic effects may play a vital role is repulsion between two coated DNA strands.

The model has neglected details of protein size and shape as well as details of the DNA polymer such as the helical geometry of major or minor groves, experimentally shown to be H-NS binding sites [3] as well as being relevant to electrostatic attraction or repulsion between two strands of DNA.

Another omitted factor is recognition of binding sites (by sequence or curvature), although simulated results are valid as H-NS is known to bind indiscriminately at high concentrations [2]. While effects of varying the parameter α (modulating sharpness or continuity of the Morse potentials along the polymer) were not analysed in this project, the model can be used to explore this. This parameter is especially relevant if the model were extended to include preferred binding sites, as the proteins reach their sites by diffusing along the polymer [2].

In addition, larger scale both with respect to time and to size of the polymer may reveal large-scale consequences of self-interaction. For example, on longer chromatin polymers, distinct clusters of condensed regions have been shown to emerge with moderate protein concentrations [8].

0.7 Conclusion

The aim of the project was to observe DNA and chromatin compaction via double-sided protein bodies. Relationships showing condensation above a threshold concentration of proteins were obtained, as well as qualitative differences in Chromatin and DNA structures that agree with expectations. The project further showed that the hypothesized return to the open state at high concentrations does not result from this size and model of protein with the forces simulated. Results could be refined and extended with a larger volume of simulations, both in terms of size of the polymer and number of repeated runs.

Bibliography

[1] R. T. Dame, "The role of nucleoid-associated proteins in the organization and compaction of bacterial chromatin," *Molecular Biology*, vol. 56(4), pp. 858–870, 2005.

[2] R. Wagner, *Transcription Regulation in Prokaryotes*. Oxford University Press, 2000.

[3] R. T. Dame, M. C. Noom, and G. J. Wuite, "Bacterial chromatin organization by h-ns protein unravelled using dual dna manipulation," *Nature*, vol. 444, no. 7117, pp. 387–390, 2006.

[4] J. R. v. d. Maarel, *Introduction to Biopolymer Physics*. World Scientific, 2007.

[5] T. Schlick, *Molecular Modeling and Simulation: An Interdisciplinary Guide*. Springer, 2 ed., 2010.

[6] S. Plimpton, "Fast parallel algorithms for short-range molecular dynamics," *J Comp Phys*, vol. 117, pp. 1–19, 1995.

[7] W. Humphrey, A. Dalke, and K. Schulten, "VMD – Visual Molecular Dynamics," *Journal of Molecular Graphics*, vol. 14, pp. 33–38, 1996.

[8] M. Barbieri, M. Chotalia, J. Fraser, L.-M. Lavitas, J. Dostie, A. Pombo, and M. Nicodemi, "Complexity of chromatin folding is captured by the strings and binders switch model," *Proceedings of the National Academy of Sciences*, vol. 109, no. 40, pp. 16173–16178, 2012.

[9] V. B. Teif and K. Bohinc, "Condensed DNA: Condensing the concepts," *Progress in Biophysics and Molecular Biology*, vol. 105, pp. 208–222, May 2011.

[10] V. B. Teif, "Ligand-induced DNA condensation: Choosing the model," *Biophysical Journal*, vol. 89, pp. 2574–2585, October 2005.